Ecotoxicology and Environmental Safety 249 (2023) 114402

Contents lists available at ScienceDirect

Ecotoxicology and Environmental Safety

journal homepage: www.elsevier.com/locate/ecoenv

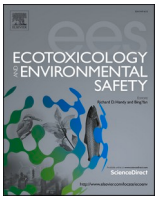

Retardation factors in controlling the transport of inorganic, organic, and particulate phosphorus in fluvo-aquic soil

Yali Chen [a], Lei Huang [a], Ran Zhang [a], Jie Ma [a,*], Zhiying Guo [b], Junying Zhao [b], Liping Weng [a,c], Yongtao Li [d]

[a] Agro-Environmental Protection Institute, Ministry of Agriculture and Rural Affairs/Key Laboratory of Original Agro-Environmental Pollution Prevention and Control, MARA/Tianjin Key Laboratory of Agro-Environment and Agro-Product Safety, Tianjin 300191, China
[b] School of Environmental Science and Safety Engineering, Tianjin University of Technology, Tianjin 300384, China
[c] Department of Soil Quality, Wageningen University, P.O. Box 47, 6700 AA Wageningen, the Netherlands
[d] College of Natural Resources and Environment, South China Agricultural University, Guangzhou 510642, China

ARTICLE INFO

Edited by Dr. Muhammad Zia-ur-Rehman

Keywords:
Phosphate
Phytic acid
Hydroxyapatite
Fraction
Retardation factor

ABSTRACT

Excessive application of fertilizers has caused a high load of phosphorus (P) in the North China Plain. The fate of P and its effects on aquatic ecosystems depend on its chemical speciation in soils. However, few studies systematically investigated the transport and retardation of different P species in the fluvo-aquic soil. In this study, the transport of inorganic P (orthophosphate, PO_4), organic P (phytic acid, PA) and particulate P (hydroxyapatite nanoparticles, nHAP) in the fluvo-aquic soil were investigated by column experiments, and their retardation from major soil components such as kaolin, $CaCO_3$, Al_2O_3, and goethite (GT) was also investigated by monitoring breakthrough curves and fitting transport models. The transport of P species in fluvo-aquic soil followed the order of PO_4 > PA > nHAP. A high fraction of increased clay and mineral particle-associated P (P-E) was observed for PO_4 and PA; while significant Ca-associated P (P-Ca) for nHAP. Under the experimental conditions, both $CaCO_3$ and GT were the most influential factors for PO_4, PA, and nHAP retention. Goethite strongly inhibited PO_4 transport due to its high PO_4 adsorption capacity, while $CaCO_3$ strongly inhibited PA transport due to its strong association with PA under alkaline conditions. Both $CaCO_3$ and GT can severely inhibit nHAP transport due to the favorable electrostatic conditions as well as the Ca^{2+} bridging effect. These results indicated that $CaCO_3$ played a key role in regulating the retention of organic P and particulate P in the calcareous soil, and also suggested the important role of Fe (hydr)oxides in controlling the transport of inorganic P, which could outcompete that of $CaCO_3$.

1. Introduction

In the Huang Huai Hai plains, fluvo-aquic soil is the main soil type, which produces about 60–80% of wheat and 35–40% of maize in China every year (Kong et al., 2014). However, due to the strong adsorption capacity of this soil type, phosphorus (P), which is an essential limiting macronutrient for all living organisms (Cordell et al., 2009), is the most important limiting element in this region (Xin et al., 2017). Thus, the supply of external P fertilizer is fundamental to realizing crop productivity. In China, the overapplication of mineral P fertilizers in pursuit of higher yields has been a common practice in wheat/maize production systems (Miao et al., 2011), and the total P input to maize fields in China was over 1527 Gg (10^9 g) in the 2000 s (Chen et al., 2018a). When in contact with the soil, the soluble and readily available inorganic P applied to the farmlands is rapidly immobilized, and only 10–20% of the applied inorganic P is made available to the crops within the season of application (Sattari et al., 2012). Meanwhile, surplus P can be transported in the runoff after rainfall, irrigation and snowmelt (Von, 2006). Thus, the environmental impact of P is mostly related to excessive discharge to natural waters, which contributes to the cultural eutrophication of water bodies throughout the world (Schindler, 2012).

The fate of P and its effects on crops and aquatic ecosystems depend on its chemical speciation. Soils generally contain many inorganic and organic P forms, but only soluble orthophosphate anions can be taken up directly via plant roots (Richardson et al., 2011). And in surface runoff and leaching waters, P may occur as dissolved, colloidal or particulate

* Corresponding author.
E-mail address: majie@caas.cn (J. Ma).

https://doi.org/10.1016/j.ecoenv.2022.114402
Received 12 August 2022; Received in revised form 16 October 2022; Accepted 6 December 2022
Available online 12 December 2022

species (Andersson et al., 2013). Orthophosphate (PO_4) is the main inorganic P form, which is the simplest and free ionic form. Phytic acid (PA), as the main organic form of P in seeds/grains (Raboy, 2003), can enter the soil via the extensive application of manure due to its low efficiency in monogastric animals (< 15% for pigs) for utilizing the P present in grains/seeds (Cunha, 2012). Thus, PA accounts for a large amount (20–80%) of P in the soil, and its content in soils is becoming higher with time (Zhao et al., 2022). "Particulate P" refer to P-containing particles, such as hydroxyapatite ($Ca_{10}(PO_4)_3(OH)_2$, HAP). In calcite-rich fluvo-aquic soils, metastable intermediate phases of calcium phosphate tend to transform to the least soluble and thermodynamically stable HAP form (Wang and Nancollas, 2008). Meanwhile, HAP nanoparticles (nHAP) has been advocated as a promising P nanofertilizer due to their higher use efficiency and reduced leaching rate (Wang et al., 2015), with extensive applications to remediate soils (Laperche et al., 1996; Liang et al., 2012; Xing et al., 2016).

Biogeochemical processes, including adsorption, precipitation, and complexation, determine the P retention or P availability in soils; and these chemical processes are highly dependent on the soil properties, such as the proportion of iron/aluminum (Fe/Al) (hydr)oxides, the amount and type of clay minerals, and the calcium carbonate content (Gerard, 2016). Iron and Al in solutions or as their (hydr)oxides can adsorb P through precipitation and ligand exchange reactions (Schoumans and Chardon, 2015), and Fe/Al (hydr)oxides have been generally recognized as vital agents in controlling P availability in soils due to their high P adsorption capacity and positive charge (Antelo et al., 2005; Ma et al., 2021; Xu et al., 2019a). For clay minerals, several investigations considered that clay minerals should be negligible P-binding constituents in soils, because of their low binding capacity (Manning and Goldberg, 1996; Pérez et al., 2014; Weng et al., 2011), however, other studies reporting clay minerals as an important P-binding constituents can also be found in the literature. Results from experimental studies performed over a time period of 70 years suggested that in most soils the role of clay minerals in P-binding could possibly outcompete Fe/Al oxides (Gerard, 2016). Xiong et al. (2022) also indicated that about 50% of the active P was adsorbed by clay minerals under their experimental conditions, and proposed the important role of clay minerals in controlling P adsorption and P species in the subtropical Alfisol with high clay mineral concentrations. With the existence of calcium carbonate, the formation of calcium-P compounds, magnesium-P compounds, and the P adsorption and precipitation by calcium carbonate could also occur, leading to high P retention in alkaline and calcareous soils (Eriksson et al., 2015; Ma et al., 2019). For example, strong P retention on calcite and Ca-kaolinite was observed, and the rate coefficient obtained by fitting a second-order kinetics equation was 30, 000-fold higher for calcite than for Ca-kaolinite (Kuo and Lotse, 1972). Lopez and Garcia (1997) also observed a similar correlation for P adsorption on calcite-rich vertisols.

Taking Fe/Al (hydr)oxides as an example, inorganic and organic P species could be absorbed by forming bidentate binuclear or monodentate mononuclear inner-sphere surface complexes (Antelo et al., 2005; Yan et al., 2014). The amount of absorbed organic P species, in terms of moles, was less than that of inorganic phosphate (Lü et al., 2017; Yan et al., 2014), suggesting that varied adsorption amounts of these P species implied different effects of Fe/Al (hydr)oxides on the transport of various P species in fluvo-aquic soil. There are limited studies on the transport of organic P, such as PA. A latest study indicated that PA could co-transport with Fe (oxyhydr)oxide, and ferrihydrite had a stronger facilitated ability for PA transport than hematite and GT (Zhao et al., 2022). For inorganic P, significant progress has been achieved in quantifying and modeling the PO_4 transport behaviors in porous media. Although a limited number of studies have been conducted to investigate the transport behaviors of nHAPs in porous media, most of these studies are confined to well-defined artificial column systems with quartz sand (Piccirillo et al., 2013; Wang et al., 2012a, 2012b, 2015) whereas only a few studies have been conducted in natural soils (Xu et al., 2019b). In addition, these studies mainly focused on environmental factors' effects on nHAP transport, such as ion strength, ion composition, and surface charge heterogeneities on the collector surfaces. As discussed above, major soil components such as Fe/Al (hydr) oxides, clay minerals, or calcium carbonate are important controlling factors in determining the environmental behavior of P, but their retardation effects on different P species in fluvo-aquic soil has not been clarified. Therefore, a systematic study is required. The objectives of this study were to: (1) evaluate the transport and retention behaviors of PO_4, PA, and nHAP in fluvo-aquic soil; (2) assess the role of Fe/Al (hydr) oxides, clay minerals, and calcium carbonate in controlling transport of different P species; (3) reveal the mechanism and dominated retardation factor for the transport of different P species. These results can provide insights into facilitating better assessments of the environmental behavior of P species and ultimately help to control the loss of P from soils.

2. Materials and methods

2.1. Soil sampling and analysis

The surface soil sample (0–20 cm) used in this study was collected from the Quzhou Experimental Station at the China Agricultural University in Handan City (Hebei Province) located in a typical fluvo-aquic soil area on the North China Plain. The collected soil sample was digested in polytetrafluoroethylene tubes by a mixture of HNO_3-HCl-HF (5:2:3). After digested, the samples were analyzed for the concentrations of P, Fe, Ca, and Al using an inductively coupled plasma optical emission spectrometer (ICP-OES, Optima 5300DV, Perkin-Elmer). The total organic carbon (TOC) of the samples were quantified using a TOC Analyzer (Analytik Jena multi N/C 3100) after removing the total inorganic carbon from the soil samples with HCl. The soil pH was measured in a 1:2.5 (w/w) soil/water suspension.

2.2. Experimental materials preparation

In this study, goethite (GT), aluminum oxide (Al_2O_3), kaolin, and calcium carbonate ($CaCO_3$) were considered primary active Fe (hydr) oxides, Al (hydr)oxides, clays, and calcium carbonate components in soils respectively. And PO_4, PA, and nHAP were to represent inorganic P, organic P and particulate P in soils respectively. Goethite was prepared using the method of Venema et al. (1998), and its preparation as well as identification are described in Chen et al. (2018b). Nanoscale hydroxyapatite was purchased from Beijing Deke Daojin Science and tTechnology Co., Ltd., and its morphology was observed by using scanning electron microscopy (SEM, Hitachi SU8010) (Fig. S1). Other experimental materials including kaolin, Al_2O_3, $CaCO_3$, PA ($C_6H_{18}O_{24}P_6$), and sodium dihydrogen phosphate (NaH_2PO_4) are all analytically pure and purchased from Sinopharm Chemical Reagent Co., Ltd.

2.3. Column experiments

Two types of column experiments, a large column experiment and a small column experiment, were performed in glass chromatography columns. The objective of the large column (25-cm long and 4-cm inner diameter) experiment was to investigate the transport characteristics and retention fractions of different P species in fluvo-aquic soil. The small column (10 cm long and 1.6 cm inner diameter) experiment was used to study the retardation factor for the transport of different P species.

The quartz sand was purchased from the Sinopharm Chemical Reagent Co., Ltd. with an average particle size of 182.2 μm. The sand was first soaked in 6 mol L^{-1} HCl for at least 24 h and then repeatedly rinsed with Milli-Q water. Four large columns were wet-packed (10% Milli-Q water, w/w) with a mixture of soil and quartz sand at a 1:1 (w:w)

proportion. After packing, three P species, including PO_4 (prepared from NaH_2PO_4), PA, and nHAP, with concentrations of 20 mg P L^{-1}, as well as Milli-Q water (control, CK) were respectively instilled in the columns' inlet with 10 pore volumes (PVs) using a peristaltic pump (LongerPump BT100-1L) in down-flow mode. The 20 mg P L^{-1} nHAP suspension was prepared by adding 0.011 g of nHAP to 100 mL of Milli-Q water, and the suspension was homogenized by stirring and then sonicating for 60 min

Following the large column experiments, the recovery of absorbed and effluent P, and distribution profiles of the P fractions in the columns were determined. The columns were dissected into 2.5 cm segments for a total of eight layers. The P concentrations in each layer were determined to obtain the absorbed P in columns, then the recovery of absorbed and effluent P was calculated based on the influent P concentration. The P fractions in each layer were extracted using the sequential extraction method proposed in Zohar et al. (2010), which was modified from the method reported in Hedley et al. (1982). The extraction method defined the P fractions as loosely sorbed on clay and mineral particles form (P-E), Fe and Al oxides associated form (P-Fe), Ca mineral associated form (P-Ca) and the residual form (P-R). The detailed procedures on the sequential P extraction were shown in Table S1, and the P-R is obtained by calculating the difference between the total P and the other three extracted P fractions. All the extracts were filtered through 0.45 μm cellulose-acetate filters after centrifuged.

The small columns were wet-packed (10% Milli-Q water, w/w) with either quartz sand (Control, CK) or with the addition of GT, Al_2O_3, kaolin, and $CaCO_3$ at different addition rates (0.1–2%). The specific packing settings can be found in Table S2. The bulk density and porosity of the packed sand were 1.59 g cm^{-3} and 0.39 cm^3 cm^{-3}, respectively. The pH of the influent solutions was adjusted to 8.0 using 1 mol L^{-1} HCl and NaOH, to mimic the pH condition of the fluvo-aquic soil. For all the small column experiments, first 10 PVs of different influent solutions with an ionic strength of 1 mmol L^{-1} NaCl were injected into columns, then 5 PVs of Milli-Q water with the same pH and ionic strength were eluted, at a constant Darcy velocity of 0.151 cm min^{-1} using a peristaltic pump in up-flow mode.

The inorganic P and nHAPs (after digestion using 6 mol L^{-1} HCl) concentrations were determined by molybdenum blue method using a UV–vis spectrophotometer (UV2700, Shimadzu) at 800 nm (Chen et al., 2015). Ascorbic acid was used as reducing agent in this method to avoid the influence of ion (such as Fe) in the solution on the detection of P. Phytic acid concentrations were determined using the ferric chloride and sulfosalicylic acid spectrophotometry method on a spectrophotometer at 505 nm (Naves et al., 2014). Duplicate samples and standard samples (both sample numbers were set as 5% of the total samples) were measured simultaneously to ensure the measurement accuracy.

2.4. Transport model and simulation

In this study, transport of inorganic and organic P were simulated using a convection-dispersion equation (CDE) model by assuming steady state flow and linear adsorption (Toride et al., 1999), first-order degradation and zero-order production were neglected due to short time of small column experiments. Then the two-site chemical non-equilibrium approach (Brusseau et al., 1991) was used to estimate the transport parameters of inorganic and organic P. For nHAP, the CDE with two kinetic retention sites (Bradford et al., 2003; Yu et al., 2013) was employed to describe its transport and retention in the column experiments. All the detailed transport models and simulations could refer to Supporting Information S4.

3. Results and discussion

3.1. Transport of different P species in fluvo-aquic soil

The fluvo-aquic soil showed a weak alkalinity with a pH of 7.69 and a low TOC content of 12.8 mg g^{-1}. The concentrations of P, Al, and Fe were 0.87, 68.9, and 23.6 mg g^{-1} respectively, and a high Ca content (31.5 mg g^{-1}) was observed in the fluvo-aquic soil, which was consistent with the elemental characteristics of this soil type (Chen et al., 2020; Ma et al., 2019).

The breakthrough curves of three different P species in the fluvo-aquic soil were presented in Fig. 1, which were plotted with the effluent P concentrations as a function of the PV. The recovery of absorbed and effluent P ranged from 118.6% to 127.3%, exhibiting a reliable extraction result. During the experiment (10 PVs), none of the P species completely broke through the soil column at an initial P concentration of 20 mg L^{-1}. Compared to the control, the first breakthrough of PO_4 was at about 1.5 PV, whereas the breakthrough of PA occurred at approximately 6 PV. However, nHAP breakthrough was not observed in the fluvo-aquic soil. Thus, the transport ability of the three P species in the fluvo-aquic soil was different, following the order of nHAP < PA < PO_4. The nHAP exhibited the lowest transport ability, which was consistent with the previous studies that nHAP was essentially immobile. In natural subsurface environments, nHAP tended to be retained owing to its high surface area and aspect ratio (Wang et al., 2011a), surface roughness and charge heterogeneity, and aggregation (Wang et al., 2011b). In addition, the mineral-associated organic matter (MOM) might further facilitate nHAP retention via mechanical straining enhanced by nanoparticle aggregation and surface deposition with MOM (Xu et al., 2019b). In soils, PA sorption to soil solid was stronger than that of the PO_4 (McKercher and Anderson, 1989), which was consistent with the easier PO_4 transport than that of PA in this study. Comparing to PO_4, PA had more negative surface charges; however, the maximum adsorption capacity of the positively charged lanthanum-bearing Al hydroxide for PO_4 (68.5 mg P g^{-1}) was about 1.9-fold higher than that for PA (36.4 mg P g^{-1}) (Xu et al., 2020). This was probably resulted from the larger molecular dimensions of PA and thereby encounter enhanced steric hindrance than that of PO_4 (Ruttenberg and Sulak, 2011; Yang et al., 2015). However, some Fe/Al (hydr)oxides (such as goethite, boehmite, hematite, and α-Al_2O_3) showed a lower adsorption capacity for PO_4 than that for organic P (including PA) in terms of mass unit (Lü et al., 2017; Yan et al., 2014). Thus, the transport and retention behaviors of P in the mixture of artificially modified quartz sands and major soil components were further investigated to understand the dominant retardation factors for each P species.

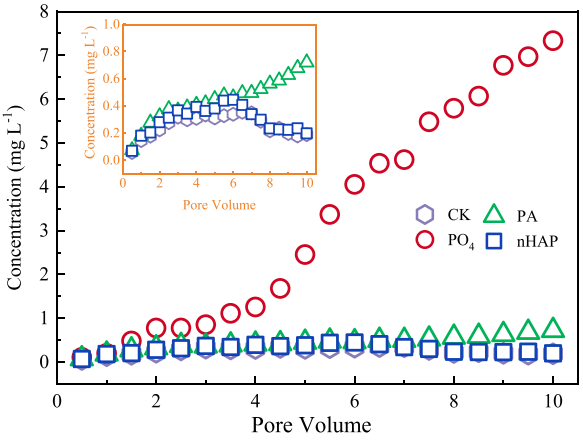

Fig. 1. Breakthrough curves of different P species in the fluvo-aquic soil (50%)-quartz sand (50%) columns at a pH of 8.0. The columns treated with Milli-Q water (CK), PO_4, PA, and nHAP were denoted by hexagons, circles, triangles, and squares, respectively.

3.2. Retention characteristics and fractions of different P species in fluvo-aquic soil

In the natural environment, the P fraction can be used to assess the potential environmental risks of P associated with plant health and groundwater pollution. Fig. 2 and S2 show the distribution of the P fractions and their increments in the columns, compared with the control. After the transport experiments, the total P contents in the columns increased by 5.87–7.73% compared with the initial soil P content; moreover, the largest increments were observed near the column inlet, especially for nHAP as shown in Fig. 2 and S2, which was consistent with the retention order of nHAP > PA > PO_4 (Fig. 2 and S2) showed in Fig. 1.

The P fractions in the soil columns all showed a similar trend of P-Ca > P-R > P-Fe > P-E (Fig. S2), which is similar to previous researches on the P fractions in calcareous soil (Jalali and Ranjbar, 2010; Ma et al., 2019). There was a notable increase in the amount of each P fraction for PO_4 and PA (Fig. 2), especially for P-E, which accounted for 60.1–63.6% of the total P increment. The $NaHCO_3$ extracted P-E, with part of the labile organic P included, represents an estimation of the P that is loosely adsorbed onto clay and mineral particles. Moreover, compared with Fe/Al (hydr)oxides, the P adsorbed onto clay minerals could be desorbed more easily, thus indicating a much more readily availability of P adsorbed onto clay minerals to plants (Al-Kanani and Mackenzie, 1991) and the high P-E fraction may pose an environmental risk for P loss to surface water and lead to eutrophication. The P-Fe and P-Ca showed similar accumulation characteristics for PO_4 and PA, and the total accumulated P-Fe and P-Ca contents for PA were higher than those for PO_4, indicating the important role of Fe/Al (hydr)oxides and $CaCO_3$ in P immobilization, especially for PA (Amini et al., 2020; Carreira et al., 2006; Celi et al., 2020; Lü et al., 2017; Ma et al., 2019). For nHAP, significant content of P-Ca increments, but negligible contents of P-E and P-Fe increments, were observed in the soil column (Fig. 2), which was possibly resulted from the particulate form of nHAP as limited active P could be absorbed by clay and Fe/Al minerals. In addition, each P fraction showed a gradual decrement from the inlet to outlet of the column for PO_4, while the gradual decrement in each P fraction for PA mainly occurred at the lower part of the column near the inlet. The P-Ca content for nHAP was most concentrated at the inlet, and the high content (up to about 245 mg/kg) could ascribe to the Ca that nHAP contained (Fig. 2), further suggesting the lowest transport ability of nHAP in fluvo-aquic soil (Fig. 1). The retention of P-R fraction fluctuated at around zero (Fig. S2) due to the determinate error, suggesting that there was no short-term residual P formation.

3.3. Retardation factor for the transport of different P species

3.3.1. Transport of PO_4

To further investigate the influence of major soil components on the transport and retardation of P species in fluvo-aquic soil columns, kaolin, $CaCO_3$, Al_2O_3, as well as GT were artificially added. The observed and simulated breakthrough curves for P transport in small columns were shown in Fig. 3. The simulation results were listed in Table 1, and most of the experimental data well fitted with the model with high r^2 values (0.65–0.87). The treatments with added GT exhibited high P retardation in columns (Fig. 3), thus the experimental data could not be fitted (such as 1% GT and 2% GT) or fitted with low r^2 value (0.34 for 0.5% GT). The derived retardation factor R quantifies the solute decrease during its transport. At a pH of 8.0, the variation magnitude in the R values for different columns was in the order of 2% $CaCO_3$ (389) > 2% Al_2O_3 (146) > 2% Soil (4.08) > CK (3.40) ≈ 2% kaolin (3.17), with $CaCO_3$ exhibited the highest inhibition ability for PO_4 transport. Meanwhile, the above mentioned order was consistent with the order of the average relative concentration (Ave C/C_0) for P in the effluent: 2% $CaCO_3$ (0.114) < 2% Al_2O_3 (0.382) < 2% Soil (0.661) < CK (0.668) ≈ 2% kaolin (0.669) (Table 1).

Although 2% GT was not fitted by the CDE model, its continuous zero C/C_0 values throughout 15 PVs suggested that Fe minerals exhibited higher inhibition ability than $CaCO_3$, considering that the release of labile P in the 2% $CaCO_3$ column was observed during the pure-water–elution period (11–15 PVs) (Fig. 3). This indicated that Fe minerals strongly inhibited PO_4 transport compared to Ca (Ma et al., 2019), and this result was consistent with the observation that PO_4 transport in the Fe-rich laterite soil was significantly slower than that in the chernozem soil and fluvo-aquic soil (Ma et al., 2021). Several researches have also shown that PO_4 adsorbed onto Fe minerals was present or even more important in neutral to calcareous soils (Beauchemin et al., 2003; Jiang et al., 2021; Ryan et al., 1985). To further investigate the inhibition abilities of Fe minerals and $CaCO_3$, different proportions of GT (0.1%−1%) and $CaCO_3$ (0.2%) were added (Fig. 3b and c). As indicated, the inhibition ability of GT and $CaCO_3$ is closely related to their addition rate. At a lower proportion (0.2%), $CaCO_3$ showed limited PO_4 inhibition with a higher Ave C/C_0 ratio (0.603) of P in the effluent; however, a relatively lower Ave C/C_0 ratio (0.341) indicated stronger inhibition from GT at an identical amount (Table 1). Meanwhile, for 0.2% GT treatment, we observed a relatively higher retardation factor R (202) as well as a lower β value (0.003) due to a decrement in the P instantaneous adsorption (Table 1). With an increase in addition rate of GT to 1%, no PO_4 was detected in the effluent (1–15 PVs); while P was observed

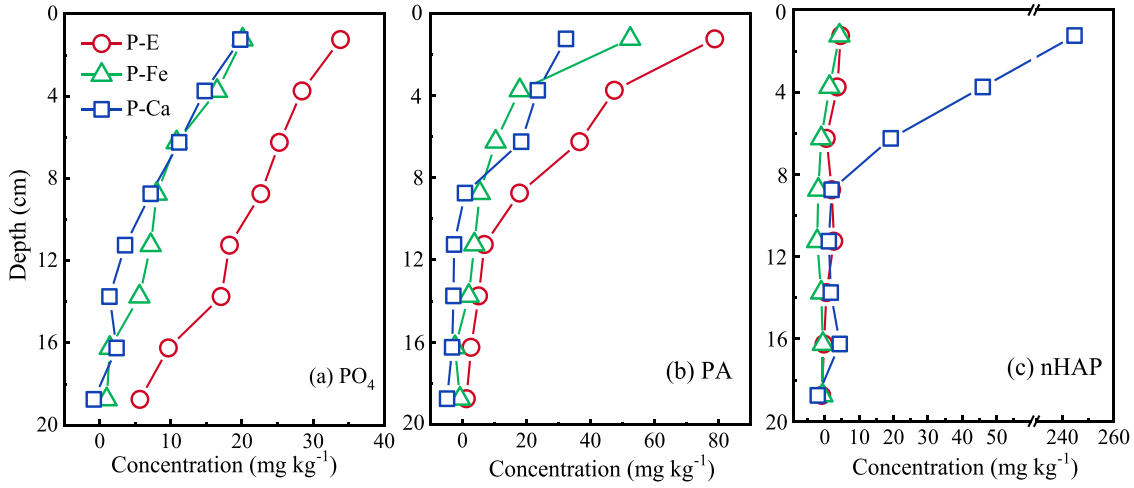

Fig. 2. Accumulated fractions of PO_4 (a), PA (b), and nHAP (c) in the fluvo-aquic soil (50%) - quartz sand (50%) columns compared with the control. The fraction distributions of different P species in the columns were shown in Fig. S2. P-E, P-Fe, and P-Ca were denoted by circles, triangles, and squares, respectively.

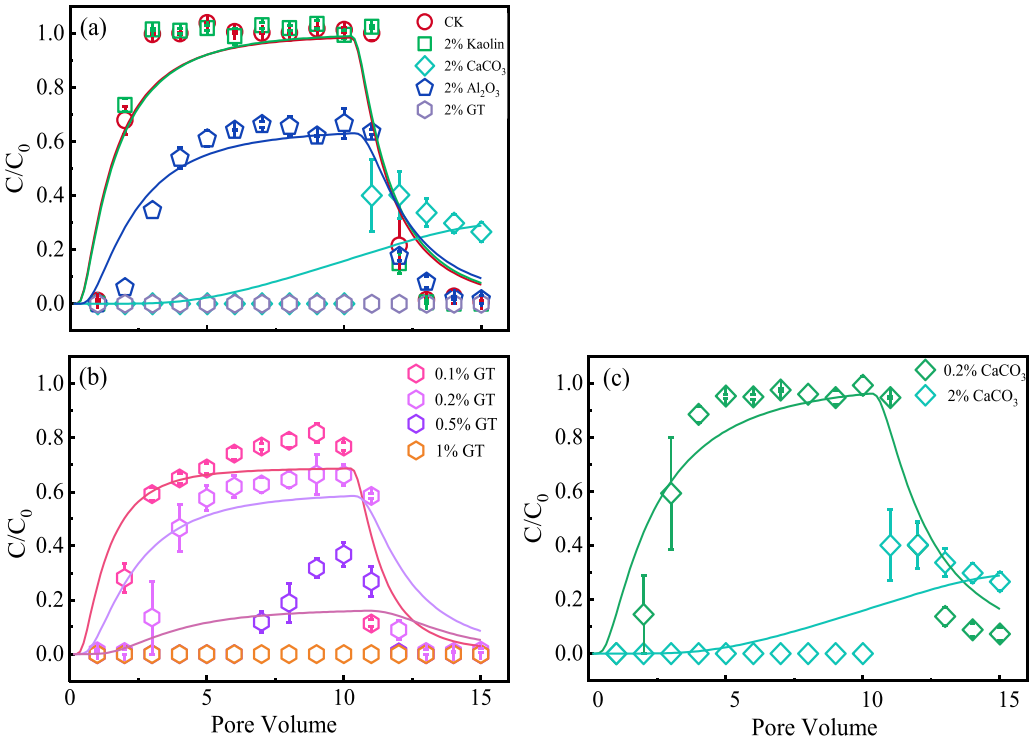

Fig. 3. Breakthrough curves of the PO_4 in quartz sand (control, CK) and quartz sand-filler mixture columns ((a)-(c)) at a pH of 8.0. Symbols show the observed data, and the solid lines show the simulation fitting. C and C_0 represented the initial concentration of P species and the concentration of P species in the effluent, respectively. Pure quartz sand (CK) was denoted by circles, and quartz sand mixed with Kaolin, $CaCO_3$, Al_2O_3 and GT were denoted by squares, rhombuses, pentagons, and hexagons, respectively.

Table 1
Experimental and fitted parameters for PO_4 transport using a two-site nonequilibrium transport model.

Index	CK	2% Kaolin	0.2% $CaCO_3$	2% $CaCO_3$	2% Al_2O_3	0.1% GT	0.2% GT	0.5% GT	1% GT	2% GT
R[a]	3.40 ± 0.13	3.17 ± 0.16	4.33 ± 0.10	389 ± 21	146 ± 3.8	158 ± 36	202 ± 42	878 ± 167	–	–
β[b]	0.93 ± 0.02	0.97 ± 0.03	0.98 ± 0.02	0.13 ± 0.01	0.04 ± 0.00	0.02 ± 0.00	0.03 ± 0.00	0.02 ± 0.00	–	–
ω[c]	0.00 ± 0.00	0.00 ± 0.00	0.15 ± 0.14	0.00 ± 0.00	0.57 ± 0.02	0.46 ± 0.03	0.69 ± 0.12	3.65 ± 0.57	–	–
Ave C/C_0[d]	0.668	0.669	0.603	0.114	0.382	0.414	0.341	0.085	0	0
r^2[e]	0.87 ± 0.00	0.86 ± 0.00	0.86 ± 0.06	0.65 ± 0.06	0.85 ± 0.01	0.83 ± 0.02	0.76 ± 0.03	0.34 ± 0.02	–	–

[a] retardation factor
[b] fraction of instantaneous retardation (dimensionless)
[c] mass transfer coefficient (dimensionless)
[d] average relative concentration
[e] correlation coefficient of the regression for the observed versus predicted data.

during the purewater–elution period (11–15 PVs) for treatment with $CaCO_3$ even added as 2%, further suggesting a stronger inhibition from Fe minerals than $CaCO_3$ in this study. Meanwhile, increasing ω values following increasing amounts of GT (Table 1) indicated a reduced sorption time for PO_4 adsorbed onto GT due to the high affinity of GT with its increasing amount.

Previous research indicated that minerals such as GT and gibbsite strongly influenced P adsorption, with GT affected most and gibbsite to a lesser extent (Oliveira et al., 2020; Xiong et al., 2022). In our study, Al_2O_3 exhibited moderate inhibition for PO_4 with an R value (146) lower than that of GT and $CaCO_3$ at a 2% addition rate; meanwhile, a relatively higher Ave C/C_0 ratio (0.382) for P in the effluent treated by 2% Al_2O_3 was observed (Table 1), which was consistent with previous research. However, in the presence of kaolin, PO_4 transport was almost not affected compared to CK, suggesting that kaolin was not a hindrance factor for PO_4 retention in soils. As previous studies indicated, the adsorption of available P onto clay minerals was extremely low even though the clays had a high surface area and CEC (Zhang et al., 2019), and desorption of the sorbed P mostly occurred via a ligand exchange reaction (Geelhoed et al., 1999; Hinsinger, 2001). Thus, the minerals most strongly inhibiting P transport was Fe (hydr)oxides GT, followed by $CaCO_3$; and the inhibition from Al (hydr)oxides Al_2O_3 was to a lesser extent.

3.3.2. *Transport of PA*

The observed and simulated breakthrough curves for PA transport with the addition of 0.2% of kaolin, $CaCO_3$, Al_2O_3, and GT at a pH of 8.0 were shown in Fig. 4, and the simulation results were listed in Table 2. As indicated, the experimental data fitted well with the model based on the high r^2 values (0.63–0.91). At pH 8.0, different PA retardations were observed with the following order: 0.2% $CaCO_3$ (R=897) > 0.2% GT (R=624) > 0.2% Al_2O_3 (R=103) > 0.2% kaolin (R=76) > CK (R=3.6), which was consistent with the observed increasing Ave C/C_0 ratios for the above components (Table 2). Thus, $CaCO_3$ and GT still played important roles in controlling PA transport, but $CaCO_3$ showed a greater retention impact.

For 0.2% $CaCO_3$, it exhibited much stronger inhibition for PA (Ave C/C_0 =0.07; R=897) than for PO_4 (Ave C/C_0 =0.60; R=4.33) (Table 1 and Table 2), further indicating that $CaCO_3$ should be the most influential factor in determining the different transport behaviors of PO_4 and PA in fluvo-aquic soil. Moreover, the high ω value (2.43) for PA transport in the $CaCO_3$ added column (Table 2) further indicated rapid adsorption due to strong inhibition from $CaCO_3$. As indicated, PA reacted readily in soils through adsorption reactions, and could form

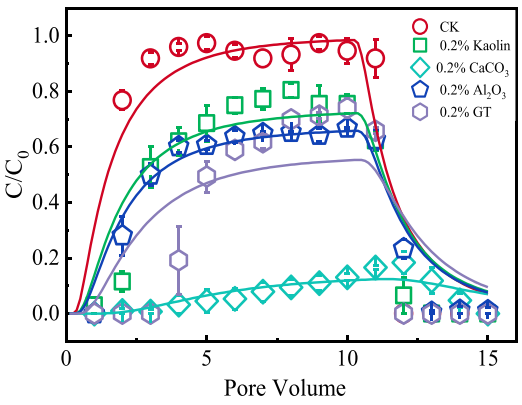

Fig. 4. Breakthrough curves of PA in the quartz sand (CK) and quartz sand-filler mixture columns at a pH of 8.0. Symbols show the observed data and solid lines show the simulation fitting. C and C_0 represented the initial concentration of P species and the concentration of P species in the effluent, respectively. Pure quartz sand (CK) was denoted by circles, and quartz sand mixed with Kaolin, $CaCO_3$, Al_2O_3 and GT were denoted by squares, rhombuses, pentagons, and hexagons, respectively.

Table 2
Experimental and fitted parameters for PA transport using the two-site nonequilibrium transport model.

Index	CK	0.2% Kaolin	0.2% $CaCO_3$	0.2% Al_2O_3	0.2% GT
R	3.60 ± 0.33	76 ± 35	897 ± 55	103 ± 16	624 ± 27
β	0.83 ± 0.08	0.07 ± 0.03	0.03 ± 0.00	0.05 ± 0.01	0.01 ± 0.00
ω	0.01 ± 0.01	0.40 ± 0.10	2.43 ± 2.40	0.52 ± 0.04	0.41 ± 0.40
Ave C/C_0	0.617	0.434	0.072	0.409	0.313
r^2	0.87 ± 0.01	0.84 ± 0.03	0.66 ± 0.04	0.91 ± 0.01	0.63 ± 0.04

precipitates with Ca in alkaline soils (Von, 2006). Beißner (1997) investigated the P acquisition from PA by sugar beet plants cultured in quartz sand, and attributed the limited P acquisition from PA than that of PO_4 to the low PA solubility even in the quartz sand system, probably owing to the formation of Ca-PA precipitates.

Under the same addition rate (0.2%), GT exhibited a slightly stronger inhibition ability for PA (Ave C/C_0 =0.31; R=624) than that of PO_4 (Ave C/C_0 =0.34; R=202) (Table 2), which was consistent with the observation that the sorption of PA was higher than that of PO_4 onto Fe (hydr) oxides such as GT and ferrihydrite (Celi and Barberis, 2005). In addition, according to McKercher and Anderson (1989), inositol sorption to soil solid was also stronger compared to that of the PO_4, and higher inositol phosphate sorption to soil solid phase would be observed with higher phosphorylation degree of the inositol ring.

For Al (hydr)oxides and clay minerals, they both exhibited stronger inhibition for PA transport than that of PO_4. Although the addition rate of Al_2O_3 and kaolin was decreased to 0.2%, the transport ability of PA was just slightly enhanced or even decreased (Table 2), compared to the PO_4 transport with 2% Al_2O_3 and kaolin (Table 1). Celi et al. (1999) indicated that clay minerals such as kaolinite and illite could retain a higher amount of P in the organic form than in the inorganic one, which could lead to a severe inhibition of PA transport from kaolin. Furthermore, the high affinity of these clay minerals for PA might result from a more stable complex (lower energy state) with their surfaces (Celi et al., 1999), with inner-sphere surface complex as major adsorbed species below pH 6 and outer-sphere surface complex as the dominant species above pH 7 (Hu et al., 2020; Ruyter-Hooley et al., 2017). However, in contrast with PO_4 transport, PA retardation from Al_2O_3 (R=103, Ave C/C_0 =0.41) and kaolin (R=76, Ave C/C_0 =0.43) exhibited limited differences, with Al_2O_3 exhibiting slightly higher inhibition for PA transport.

In general, PA transport was not favored in the presence of major fluvo-aquic soil components such as Fe/Al (hydr)oxides, $CaCO_3$, and clays, and the preferential retain or accumulation of PA in soils could be attributed to its strong interaction with these soil components. In our study, PA transport in all the columns except CK, the β values (which represent the ratio of instantaneous retardation to total retardation) (Florido et al., 2010) were all very small (0.01–0.07, Table 2), revealing that a larger amount of PA was adsorbed at nonequilibrium sites rather than at equilibrium sites. Different from PO_4, $CaCO_3$ strongly inhibited PA transport, with Fe (hydr)oxides GT, Al (hydr)oxides Al_2O_3 and kaolin to a lesser extent.

3.3.3. *Transport of nHAP*

Similarly, we investigated the transport of nHAP in columns mixed with 0.2% kaolin, $CaCO_3$, Al_2O_3, and GT at a pH of 8.0. The breakthrough curves and simulation results were shown in Fig. 5, and the fitted parameters for nHAP transport were summarized in Table 3. The experimental data fitted well with the model, as indicated by the high r^2 values (r^2 = 0.87–0.95). However, for columns with $CaCO_3$ and GT, due to the strong inhibition of nHAP transport in these columns (Ave C/C_0 = 0.042 and 0.051, Table 3), the experimental data were fitted with low r^2 values (r^2 = 0.41 and 0.40).

The transport ability of nHAP decreased as the following order: CK > 0.2% kaolin > 0.2% Al_2O_3 > 0.2% GT > 0.2% $CaCO_3$ (Fig. 5), which was consistent with the order of the Ave C/C_0 of P in the effluent (0.042–0.232, Table 3). Compared to CK (k_{2a}: 0.74; k_{1d}/k_{1a}: 0.45), all the treatments exhibited relatively higher k_{2a} (0.79–2.00) and lower k_{1d}/k_{1a} (0.01–0.43) values, and the magnitude of k_{2a} and k_{1d}/k_{1a} also varied accordingly with the Ave C/C_0 values (Table 3). The higher values of k_{2a} indicated increased irreversible retention of nHAP, and the smaller k_{1d}/k_{1a} ratios further indicated the increased nHAP retention on time-dependent sites, suggesting the attachment interaction between nHAP and the collector was stronger than detachment. In general, $CaCO_3$ exhibited the highest retardation of nHAP transport among different treatments, followed by GT. And this phenomenon could be caused by the presence of favorable surfaces (i.e., favorable attachment conditions) for nHAP attachment (Wang et al., 2012a). At ambient pH values, nHAP, as well as major soil components, such as silica and clay minerals, exhibited net negative surface charges (D'Amora et al., 2020;

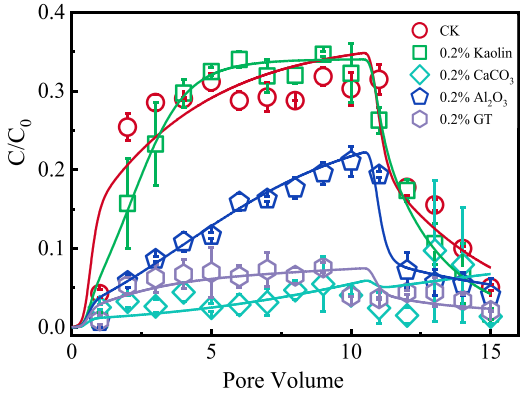

Fig. 5. Breakthrough curves for nHAP in the quartz (CK) sand quartz sand-filler mixture columns at a pH of 8.0. Symbols show the observed data and solid lines show the simulation fitting. C and C_0 represented the initial concentration of P species and the concentration of P species in the effluent, respectively. Pure quartz sand (CK) was denoted by circles, and quartz sand mixed with Kaolin, $CaCO_3$, Al_2O_3 and GT were denoted by squares, rhombuses, pentagons, and hexagons, respectively.

Table 3
Experimental and fitted parameters for nHAP transport using the two-site kinetic model.

Index	CK	0.2% Kaolin	0.2% $CaCO_3$	0.2% Al_2O_3	0.2% GT
k_{1a}[a]	0.12 ± 0.01	0.35 ± 0.15	0.68 ± 0.13	0.29 ± 0.00	0.24 ± 0.01
k_{1d}[b]	0.05 ± 0.01	0.11 ± 0.03	0.01 ± 0.01	0.02 ± 0.01	0.01 ± 0.01
k_{2a}[c]	0.74 ± 0.05	0.79 ± 0.01	2.00 ± 0.41	1.00 ± 0.12	1.63 ± 0.40
k_{1d}/ k_{1a}	0.45 ± 0.05	0.43 ± 0.28	0.01 ± 0.01	0.06 ± 0.04	0.04 ± 0.02
S_{max2}[d]	17,329 ± 7322	12.4 ± 12.0	53.2 ± 34.6	0.74 ± 0.01	35.2 ± 35.0
Ave C/ C_0	0.232	0.220	0.042	0.113	0.051
r^2	0.87 ± 0.00	0.95 ± 0.03	0.41 ± 0.07	0.90 ± 0.05	0.40 ± 0.17

[a] first-order retention coefficient on Site-1
[b] first-order detachment coefficient on Site-1
[c] first-order retention coefficient on Site-2
[d] maximum colloid concentration on Site-2.

Wang et al., 2011b), whereas $CaCO_3$, as well as Fe and Al oxyhydroxides, showed net positive surface charges due to their relatively high points of zero charge (PZC) (Abudalo et al., 2010; Johnson et al., 1996). Thus, nHAP attachment should be "unfavorable" for negatively charged collectors and "favorable" for positively charged collectors (Wang et al., 2012a). However, nHAP did not show high transport ability in the pure quartz sand (CK) or kaolin-mixed sand columns (Ave $C/C_0 \approx 0.23$, Table 3). Previous studies suggested that nHAP aggregation, nHAP surface charge heterogeneity, and roughness of the collector surface were significant factors in controlling nHAP retention in pure quartz sands (Wang et al., 2012a, 2012b). In Fe oxide-coated sand column, a significant amount of nHAP attachment was observed compared with CK as a result of the favorable electrostatic conditions between the negatively charged nHAP and positively charged Fe oxide surfaces (Wang et al., 2012a, 2012b). Similarly, in this study, a much stronger nHAP retardation was observed in the columns containing positively charged Al_2O_3 and $CaCO_3$. Comparing to the PZC for Al_2O_3 (9, refer to Wang et al., 2012a), the higher PZC for GT (9.3) led to stronger electrostatic interaction between GT and nHAP, further resulting in stronger nHAP retardation. For $CaCO_3$, except for electrostatic interactions, the Ca^{2+} released at a pH of 8 could act as a bridging agent, resulting in larger nHAP aggregate formation (Wang et al., 2011a), thereby severely inhibiting nHAP transport. Thus, compared to PO_4 and PA, nHAP exhibited the lowest transport ability. For nHAP, $CaCO_3$ strongly inhibited its transport, followed by Fe (hydr)oxides GT and Al (hydr) oxides Al_2O_3, with kaolin to a lesser extent.

3.3.4. *Importance of $CaCO_3$ and GT for retention of different P species*

The fate of P in the soil is controlled by P species, which varies with soil compositions. The contributions of individual soil constituents for the retention of P species during their transport in the fluvo-aquic soil can be evaluated by comparing their transport abilities. As mentioned above, the P species determined the P transport ability in fluvo-aquic soil, following the order of $PO_4 > PA > nHAP$. Under the conducted experiment conditions, $CaCO_3$ and GT were the most influential retardation factors for PO_4, PA, and nHAP transport, but they showed varied inhibition abilities even at identical addition rate.

As shown in Table S3, in comparison to the CK, 0.2% GT exhibited similar inhibition (by ~49%) for both PO_4 and PA, while 0.2% $CaCO_3$ showed significant inhibition (by 88.3%) for PA but only limited inhibition (by 9.7%) for PO_4, indicating that $CaCO_3$ determined the different retention behaviors of PO_4 and PA in soils. However, nHAP transport was strongly inhibited both by both $CaCO_3$ (81.9%) and GT (78.0%), further suggesting that the strong retention of nHAP in soils resulted from the combined inhibition effects of $CaCO_3$ and GT, with a slightly higher contribution from $CaCO_3$. Thus, it can be deduced that $CaCO_3$ determined the different transport behaviors between PO_4 and PA while GT determined those between nHAP and PA; both $CaCO_3$ and GT determined the varied transport behaviors between PO_4 and nHAP, with higher contributions from $CaCO_3$.

4. Conclusions

As the dominant P species in soils, PO_4, PA, and nHAP exhibited different transport abilities in the order of $PO_4 > PA > nHAP$ in fluvo-aquic soil. Approximately 60% of the retained P was in the P-E form for PO_4 and PA, while about 95% of the retained P was in the P-Ca form for nHAP. Compared to the control, GT strongly inhibited PO_4 transport (by 49.0%) whereas $CaCO_3$ transport was only inhibited by 9.7%; similar GT inhibition (by 49.3%) but much stronger $CaCO_3$ inhibition (by 88.3%) was observed for PA; and both $CaCO_3$ (81.9%) and GT (78.0%) exhibited strong inhibition for nHAP transport. Our results indicated that $CaCO_3$ played a key role in regulating the P retention in the calcareous soil such as fluvo-aquic soil, especially for organic P and particulate P. Moreover, the role of Fe (hydr)oxides in controlling inorganic P transport could outcompete that of $CaCO_3$, which implied a limit inorganic P transport/loss in the Fe-rich soil, such as laterite soil. This study provided a comprehensive perspective for the assessment of retardation factors for the transport and retention of different P species in fluvo-aquic soil.

CRediT authorship contribution statement

Yali Chen: Data curation, Writing – original draft, Writing – review & editing, Funding acquisition. **Lei Huang**: Resources, Investigation, Formal analysis. **Ran Zhang**: Formal analysis, Writing – review & editing. **Jie Ma**: Conceptualization, Methodology, Writing – review & editing. **Zhiying Guo**: Investigation, Formal analysis. **Junying Zhao**: Writing – review & editing. **Liping Weng**: Funding acquisition, Writing – review & editing. **Yongtao Li**: Writing – review & editing.

Declaration of Competing Interest

The authors declare that they have no known competing financial interests or personal relationships that could have appeared to influence the work reported in this paper.

Data availability

The data that has been used is confidential.

Acknowledgments

This study is financially supported by the Key Projects at the Institute of Innovation Engineering, the National Key Research and Development Program of China (2021YFD1700904), the Central Public-interest Scientific Institution Basal Research Fund (2022-jbkyywf-cyl), and the National Key Research and Development Program of China (2016YFD0800102).

Appendix A. Supporting information

Supplementary data associated with this article can be found in the online version at doi:10.1016/j.ecoenv.2022.114402.

References

Abudalo, R.A., Ryan, J.N., Harvey, R.W., Metge, D.W., Landkamer, I., 2010. Influence of organic matter on the transport of Cryptosporidium parvum oocysts in a ferric

oxyhydroxide-coated quartz sand saturated porous medium. Water Res. 44, 1104–1113.
Al-Kanani, T., Mackenzie, A.F., 1991. Sorption and desorption of orthophosphate and pyrophosphate by mineral fractions of soils, goethite, and kaolinite. Can. J. Soil Sci. 71, 327–338.
Amini, M., Antelo, J., Fiol, S., Rahnemaie, R., 2020. Modeling the effects of humic acid and anoxic condition on phosphate adsorption onto goethite. Chemosphere 253, 126691.
Andersson, H., Bergström, L., Djodjic, F., Ulén, B., Kirchmann, H., 2013. Topsoil and subsoil properties influence phosphorus leaching from four agricultural soils. J. Environ. Qual. 42, 455–463.
Antelo, J., Avena, M., Fiol, S., Lopez, R., Arce, F., 2005. Effects of pH and ionic strength on the adsorption of phosphate and arsenate at the goethiteewater interface. J. Colloid Interface Sci. 285, 476–486.
Beauchemin, S., Hesterberg, D., Chou, J., Beauchemin, M., Simard, R.R., Sayers, D.E., 2003. Speciation of phosphorus in phosphorus-enriched agricultural soils using X-ray absorption near-edge structure spectroscopy and chemical fractionation. J. Environ. Qual. 32, 1809–1819.
Beißner, L., 1997. Mobilisierung von Phosphor aus Organischen und Anorganischen Verbindungen Durch Zuckerrübenwurzeln. Georg-August Universität, Göttingen, Germany.
Bradford, S.A., Simunek, J., Bettahar, M., Van Genuchten, M.T., Yates, S.R., 2003. Modeling colloid attachment, straining, and exclusion in saturated porous media. Environ. Sci. Technol. 37, 2242–2250.
Brusseau, M.L., Jessup, R.E., Rao, P.S.C., 1991. Nonequilibrium sorption of organic chemicals: elucidation of rate-limiting processes. Environ. Sci. Technol. 25, 1334-1334.
Carreira, J., Viñegla, B., Lajtha, K., 2006. Secondary $CaCO_3$ and precipitation of P–Ca compounds control the retention of soil P in arid ecosystems. J. Arid Environ. 64, 460–473.
Celi, L., Lamacchia, S., Marsan, F.A., Barberis, E., 1999. Interaction of inositol hexaphosphate on clays: adsorption and charging phenomena. Soil Sci. 164, 574–585.
Celi, L., Prati, M., Magnacca, G., Santoro, V., Martin, M., 2020. Role of crystalline iron oxides on stabilization of inositol phosphates in soil. Geoderma 374, 114442.
Celi, L.R., Barberis, E., 2005. Abiotic stabilization of organic phosphorus in the environment. In: Turner, B.L., Frossard, E., Baldwin, D.S. (Eds.), Organic Phosphorus in the Environment. CABI Publishing, Wallingford, UK, pp. 113–132.
Chen, M., Xu, N., Cao, X., Zhou, K., Chen, Z., Wang, Y., Liu, C., 2015. Facilitated transport of anatase titanium dioxides nanoparticles in the presence of phosphate in saturated sands. J. Colloid Interface Sci. 451, 134–143.
Chen, X., Ma, L., Ma, W., Wu, Z., Cui, Z., Hou, Y., Zhang, F., 2018a. What has caused the use of fertilizers to skyrocket in China? Nutr. Cycl. Agroecosyst. 110, 241-225.
Chen, Y., Ma, J., Li, Y., Weng, L., 2018b. Enhanced cadmium immobilization in saturated media by gradual stabilization of goethite in the presence of humic acid with increasing pH. Sci. Total Environ. 648, 358–366.
Chen, Y., Ma, J., Wu, X., Weng, L., Li, Y., 2020. Sedimentation and transport of different soil colloids: effects of goethite and humic acid. Water 12, 1–14.
Cordell, D., Drangert, J.O., White, S., 2009. The story of phosphorus: global food security and food for thought. Glob. Environ. Change 19, 292–305.
Cunha, T., 2012. Swine Feeding and Nutrition. Academic Press, New York, USA.
D'Amora, M., Liendo, F., Deorsola, F.A., Bensaid, S., Giordani, S., 2020. Toxicological profile of calcium carbonate nanoparticles for industrial applications. Colloids Surf. B Biointerfaces 190, 110947.
Eriksson, A.K., Gustafsson, J.P., Hesterberg, D., 2015. Phosphorus speciation of clay fractions from long-term fertility experiments in Sweden. Geoderma 241–242, 68–74.
Florido, A., Valderrama, C., Arévalo, J.A., Casas, I., Martínez, M., Miralles, N., 2010. Application of two sites non-equilibrium sorption model for the removal of Cu(II) onto grape stalk wastes in a fixed-bed column. Chem. Eng. J. 156, 298–304.
Gérard, F., 2016. Clay minerals, iron/aluminum oxides, and their contribution to phosphate sorption in soils — a myth revisited. Geoderma 262, 213–226.
Geelhoed, J.S., Van Riemsdijk, W.H., Findenegg, G.R., 1999. Simulation of the effect of citrate exudation from roots on the plant availability of phosphate adsorbed on goethite. Eur. J. Soil Sci. 50, 379–390.
Gerard, F., 2016. Clay minerals, iron/aluminum oxides, and their contribution to phosphate sorption in soils. A myth revisited. Geoderma 262, 213–226.
Hedley, M.J., Stewart, J.W.B., Chauhan, B.S.C., B, S., 1982. Changes in inorganic and organic soil phosphorus fractions induced by cultivation practices and by laboratory incubations. Soil Sci. Soc. Am. J. 46, 970–976.
Hinsinger, P., 2001. Bioavailability of soil inorganic P in the rhizosphere as affected by root-induced chemical changes: a review. Plant Soil 237, 173–195.
Hu, Z., Jaisi, D.P., Yan, Y.P., Chen, H.F., Wang, X.M., Wan, B., Liu, F., Tan, W.F., Huang, X.Y., Feng, X.H., 2020. Adsorption and precipitation of *myo*-inositol hexakisphosphate onto kaolinite. Eur. J. Soil Sci. 71, 226–235.
Jalali, M., Ranjbar, F., 2010. Aging effects on phosphorus transformation rate and fractionation in some calcareous soils. Geoderma 155, 101–106.
Jiang, X., Livi, K.J.T., Arenberg, M.R., Chen, A., Arai, Y., 2021. High flow event induced the subsurface transport of particulate phosphorus and its speciation in agricultural tile drainage system. Chemosphere 263, 128147.
Johnson, P.R., Sun, N., Elimelech, M., 1996. Colloid transport in geochemically heterogeneous porous media: modeling and measurements. Environ. Sci. Technol. 30, 3284–3293.
Kong, X.B., Lal, R., Li, B.G., Liu, H.B., Li, K.J., Feng, G.L., Zhang, Q.P., Zhang, B.B., 2014. Fertilizer intensification and its impacts in China's HHH plains. Adv. Agron. 145, 235-169.
Kuo, S., Lotse, E.G., 1972. Kinetics of phosphate adsorption by calcium carbonate and Ca-kaolinite. Soil Sci. Soc. Am. J. 36, 725–729.
Laperche, V., Traina, S.J., Gaddam, P., Logan, T.J., 1996. Chemical and mineralogical characterizations of Pb in a contaminated soil: reactions with synthetic apatite. Environ. Sci. Technol. 30, 3321–3326.
Liang, Y., Wang, X., Cao, X., 2012. Immobilization of heavy metals in contaminated soils with phosphate-, carbonate-,and silicate-based amendments: a review. Environ. Chem. 31, 16–25.
Lopez, P.A., Garcia, N.A., 1997. Phosphate sorption in vertisols of southwestern Spain. Soil Sci. 162, 69–77.
Lü, C., Yan, D., He, J., Zhou, B., Li, L., Zheng, Q., 2017. Environmental geochemistry significance of organic phosphorus: an insight from its adsorption on iron oxides. Appl. Geochem. 84, 52–60.
Ma, J., Ma, Y., Wei, R., Chen, Y., Weng, L., Ouyang, X., Li, Y., 2021. Phosphorus transport in different soil types and the contribution of control factors to phosphorus retardation. Chemosphere 276, 130012.
Ma, Y., Ma, J., Peng, H., Weng, L., Chen, Y., Li, Y., 2019. Effects of iron, calcium, and organic matter on phosphorus behavior in fluvo-aquic soil: farmland investigation and aging experiments. J. Soils Sediment. 19, 3994–4004.
Manning, B.A., Goldberg, S., 1996. Modeling arsenate competitive adsorption on kaolinite, montmorillonite and illite. Clays Clay Miner. 44, 609–623.
McKercher, R., Anderson, G., 1989. Organic phosphate sorption by neutral and basic soils. Commun. Soil Sci. Plant Anal. 20, 723–732.
Miao, Y., Stewart, B.A., Fusuo, Z., 2011. Long-term experiments for sustainable nutrient management in China. A review. Agron. Sustain. Dev. 31, 397–414.
Naves, L., Rodrigues, P.B., Bertechini, A.G., Corrêa, A., Oliveira, D., Oliveira, E., Duarte, W.F., Cunha, M., 2014. Comparison of methodologies to quantify phytate phosphorus in diets containing phytase and excreta from broilers. Asian-Australas. J. Anim. Sci. 27, 1003–1012.
Oliveira, J., Inda, A.V., Barrón, V., Torrent, J., Camargo, F., 2020. Soil properties governing phosphorus adsorption in soils of Southern Brazil. Geoderma Reg., e00318
Pérez, C., Antelo, J., Fiol, S., Arce, F., 2014. Modelling oxyanion adsorption on ferralic soil, part 1: parameter validation with phosphate ion. Environ. Toxicol. Chem. 33, 2208–2216.
Piccirillo, C., Dunnill, C.W., Pullar, R.C., Tobaldi, D.M., Labrincha, J.A., Parkin, I.P., Pintado, M.M., Castro, P.M.L., 2013. Calcium phosphate-based materials of natural origin showing photocatalytic activity. J. Mater. Chem. A 1, 6452–6461.
Raboy, V., 2003. Myo-Inositol-1,2,3,4,5,6-hexakisphosphate. Phytochemistry 64, 1033–1043.
Richardson, A.E., Lynch, J.P., Ryan, P.R., Delhaize, E., Smith, F.A., Smith, S.E., Harvey, P.R., Ryan, M.H., Veneklaas, E.J., Lambers, H., Oberson, A., Culvenor, R.A., Simpson, R.J., 2011. Plant and microbial strategies to improve the phosphorus efficiency of agriculture. Plant Soil 349, 121–156.
Ruttenberg, K.C., Sulak, D.J., 2011. Sorption and desorption of dissolved organic phosphorus onto iron (oxyhydr)oxides in seawater. Geochim. Cosmochim. Acta 75, 4095–4112.
Ruyter-Hooley, M., Johnson, B.B., Morton, D.W., Angove, M.J., 2017. The adsorption of *myo*-inositol hexaphosphate onto kaolinite and its effect on cadmium retention. Appl. Clay Sci. 135, 405–413.
Ryan, J., Curtin, D., Cheema, M.A., 1985. Significance of iron oxides and calcium carbonate particle size in phosphate sorption by calcareous soils. Soil Sci. Soc. Am. J. 49, 401–414.
Sattari, S.Z., Bouwman, A.F., Giller, K.E., van Ittersum, M.K., 2012. Residual soil phosphorus as the missing piece in the global phosphorus crisis puzzle. Proc. Natl. Acad. Sci. USA 109, 6348–6353.
Schindler, D.W., 2012. The dilemma of controlling cultural eutrophication of lakes. Proc. R. Soc. B Biol. Sci. 279, 4322–4333.
Schoumans, O.F., Chardon, W.J., 2015. Phosphate saturation degree and accumulation of phosphate in various soil types in The Netherlands. Geoderma 237–238, 325–335.
Toride, N., Leij, F.J., van Genuchten, M.T., 1999. The CXTFIT Code for Estimating Transport Parameters from Laboratory or Field Tracer Experiments. U.S. Salinity Laboratory, Riverside, CA.
Venema, P., Hiemstra, T., Weidler, P.G., van Riemsdijk, W.H., 1998. Intrinsic proton affinity of reactive surface groups of metal (hydr)oxides: application to iron (hydr) oxides. J. Colloid Interface Sci. 198, 282–295.
Von, Wandruszka, R., 2006. Phosphorus retention in calcareous soils and the effect of organic matter on its mobility. Geochem. Trans. 7, 1–8.
Wang, D., Chu, L., Paradelo, M., Peijnenburg, W.J.G.M., Wang, Y., Zhou, D., 2011a. Transport behavior of humic acid-modified nano-hydroxyapatite in saturated packed column: effects of Cu, ionic strength, and ionic composition. J. Colloid Interface Sci. 360, 398–407.
Wang, D., Paradelo, M., Bradford, S.A., Peijnenburg, W.J.G.M., Chu, L., Zhou, D., 2011b. Facilitated transport of Cu with hydroxyapatite nanoparticles in saturated sand: effects of solution ionic strength and composition. Water Res. 45, 5905–5915.
Wang, D., Bradford, S.A., Harvey, R.W., Gao, B., Cang, L., Zhou, D., 2012a. Humic acid facilitates the transport of ARS-labeled hydroxyapatite nanoparticles in iron oxyhydroxide-coated sand. Environ. Sci. Technol. 46, 2738–2745.
Wang, D., Bradford, S.A., Harvey, R.W., Hao, X., Zhou, D., 2012b. Transport of ARS-labeled hydroxyapatite nanoparticles in saturated granular media is influenced by surface charge variability even in the presence of humic acid. J. Hazard. Mater. 229–230, 170–176.
Wang, D., Jin, Y., Jaisi, D.P., 2015. Cotransport of hydroxyapatite nanoparticles and hematite colloids in saturated porous media: mechanistic insights from mathematical modeling and phosphate oxygen isotope fractionation. J. Contam. Hydrol. 182, 194–209.

Wang, L., Nancollas, G.H., 2008. Calcium orthophosphates: crystallization and dissolution. Chem. Rev. 40, 4628–4669.
Weng, L.P., Vega, F.A., Van Riemsdijk, W.H., 2011. Competitive and synergistic effects in ph dependent phosphate adsorption in soils: LCD modeling. Environ. Sci. Technol. 45, 8420–8428.
Xin, X., Qin, S., Zhang, J., Zhu, A., Yang, W., Zhang, X., 2017. Yield, phosphorus use efficiency and balance response to substituting long-term chemical fertilizer use with organic manure in a wheat-maize system. Field Crops Res. 208, 27–33.
Xing, J., Hu, T., Cang, L., Zhou, D., 2016. Remediation of copper contaminated soil by using different particle sizes of apatite: a field experiment. Springerplus 5, 1182.
Xiong, J., Liu, Z., Yan, Y., Xu, J., Liu, D., Tan, W., Feng, X., 2022. Role of clay minerals in controlling phosphorus availability in a subtropical Alfisol. Geoderma 409, 115592.
Xu, J., Koopal, L.K., Wang, M., Xiong, J., Tan, W.F., 2019a. Phosphate speciation on Al-substituted goethite: ATR-FTIR/2D-COS and CD-MUSIC modeling. Environ. Sci. Nano.
Xu, R., Tao, L., Zhang, M., Cooper, M., Pan, G., 2020. Molecular-level investigations of effective biogenic phosphorus adsorption by a lanthanum/aluminum-hydroxide composite. Sci. Total Environ. 725, 138424.
Xu, S., Chen, X., Zhuang, J., 2019b. Opposite influences of mineral-associated and dissolved organic matter on the transport of hydroxyapatite nanoparticles through soil and aggregates. Environ. Res. 171, 153–160.
Yan, Y.P., Liu, F., Li, W., Liu, F., Feng, X.H., Sparks, D.L., 2014. Sorption and desorption characteristics of organic phosphates of different structures on aluminium (oxyhydr) oxides. Eur. J. Soil Sci. 65, 308–317.
Yang, Y.P., Koopal, L.K., Li, W., Zheng, A.M., Yang, J., Liu, F., Feng, X.H., 2015. Size-dependent sorption of myo-inositol hexakisphosphate and orthophosphate on nano-gamma-Al_2O_3. J. Colloid Interface Sci. 451, 85–92.
Yu, B., Jia, S.Y., Liu, Y., Wu, S.H., Han, X., 2013. Mobilization and re-adsorption of arsenate on ferrihydrite and hematite in the presence of oxalate. J. Hazard. Mater. 262, 701–708.
Zhang, L., Hu, Y., Han, F., Wu, Y., Tian, D., Su, M., Wang, S., Li, Z., Hu, S., 2019. Influences of multiple clay minerals on the phosphorus transport driven by *Aspergillus niger*. Appl. Clay Sci. 177, 12–18.
Zhao, K., Tufail, S., Arai, Y., Sharma, P., Zhang, Q., Chen, Y., Wang, X., Shang, J., 2022. Effect of phytic acid and morphology on Fe (oxyhydr)oxide transport under saturated flow condition. J. Hazard. Mater. 424, 127659.
Zohar, I., Shaviv, A., Klass, T., Roberts, K., Paytan, A., 2010. Method for the analysis of oxygen isotopic composition of soil phosphate fractions. Environ. Sci. Technol. 44, 7583–7588.